Organic Electronics 74 (2019) 161–165

Contents lists available at ScienceDirect

Organic Electronics

journal homepage: www.elsevier.com/locate/orgel

Electrically tunable dual-wavelength organic laser based on holographic polymer dispersed liquid crystal grating

Lijuan Liu[a,*], Xiaobo Kong[a], Yanqing Liu[a], Lin Sun[a], Li Xuan[b]

[a] School of Physics and Physical Engineering, Shandong Provincial Key Laboratory of Laser Polarization and Information Technology, Qufu Normal University, 273165, Qufu, China

[b] State Key Laboratory of Applied Optics, Changchun Institute of Optics, Fine Mechanics and Physics, Chinese Academy of Sciences, Changchun, 130033, China

ARTICLE INFO

Keywords:
Dual-wavelength laser
Electrically tunable
Low threshold
Holographic polymer dispersed liquid crystal grating

ABSTRACT

An organic dual-wavelength surface-emitting distributed feedback (DFB) laser with low threshold and high conversion efficiency based on holographic polymer dispersed liquid crystal (HPDLC) grating is reported. In such a laser configuration, the dye blend 4-(dicyanomethylene)-2-methyl-6-(*p*-dimethylaminostyryl)-4H-pyran (DCM)/1,3,5,7,8-pen- tamethyl-2,6-diethylpyrromethene-difluoroborate (PM567) -doped HPDLC grating is formed on the top of an organic semiconductor poly(2-methoxy-5-(20 -ethyl-hexyloxy)-p- phenylenevinylene) (MEH-PPV) layer. The dual-wavelength laser located at 605.2 nm and 629.8 nm are obtained in a single beam. The dual-wavelength laser performance under an external electric field are investigated and illustrated for the first time. This study provides some new ideas for the improvement of tunable dual-wavelength laser and extends more applications in laser displays and integrated photonic circuits.

1. Introduction

In recent years, dual-wavelength lasers (DWLs) have attracted wide attention due to their potential application prospects in precision spectroscopy, wavelength division multiplexing, THz frequency generators, medical equipment [1–3]. Previous reports on DWLs are mainly achieved by Nd-doped crystals or inorganic semiconducting materials [4–6]. Both of these two DWLs are requesting by many other fittings, which would inevitably induce optical instability and a bulky configuration. On the other hand, organic materials, including laser dyes and organic semiconductors, have the advantages of simple process, wide absorption spectrum, chemically tunable emission spectrum, good flexibility and low cost [7–9]. Compared with inorganic DWLs, organic DWLs have good optical stability and compact structure [10,11]. Specially, DWLs with electrically tunable properties have more advantages [12,13]. To achieve an electrically controllable laser, a promising and efficient way is to incorporate nematic liquid crystals (LCs) in laser resonator cavity [14–17]. Nematic LCs are electro-optical birefringent materials that their orientation can be changed by external electric field, and thus the lasing performance (e.g., lasing wavelength or intensity) can be easily modulated without moving the sample or altering the pumping setup [18]. A HPDLC grating containing alternating polymer-rich and LC-rich lamellae, is an excellent DFB configuration cavity because of its ease of preparation, low optical scattering and large processing area [19]. Distributed feedback laser action has been emitted from dyes [20] or organic semiconductors [21] based on HDPLC grating, and electrical switching of laser action in HDPLCs has also been demonstrated [14,18], but few reports have been devoted to the electrical control of the DWLs using HDPLC gratings as cavities.

In this paper, we present the electrical control of the organic DWLs based on HPDLC gratings for the first time. A dual-wavelength emission at 605.2 nm and 629.8 nm is generated by DCM/PM567 and MEH-PPV respectively in one laser beam. Compared with the earlier works [22], the laser thresholds for both laser are halved due to the rubbed polyimide (PI) layer and the location of output wavelengths. Meanwhile, the lasing performance from dye blend also could be improved due to the effective Forster energy transfer from host dye PM567 to guest dye DCM. The lasing intensity and wavelength were modulated under electric field. The results were attributed to the decreases in the refractive index difference and average refractive index of the HPDLC grating respectively, which were induced by the re-orientation of LCs under external electric field.

2. Experimental

Fig. 1a shows the fabrication process of our organic DWLs. MEH-PPV layer (molecular weight ~120000; Jilin OLED Material Company) was spin-coated (2000 rpm; 30 s) on a clean ITO (indium-tin-oxide)

* Corresponding author.
E-mail address: llj2007weihai@163.com (L. Liu).

https://doi.org/10.1016/j.orgel.2019.07.012
Received 26 May 2019; Received in revised form 5 July 2019; Accepted 5 July 2019
Available online 06 July 2019

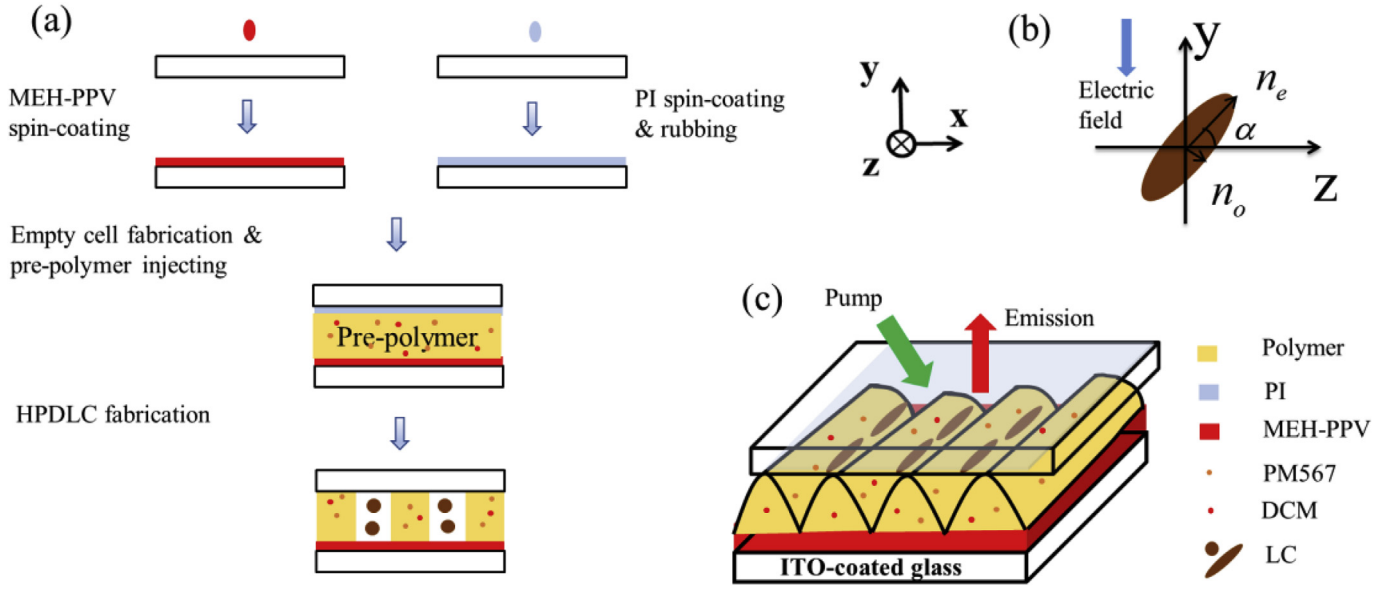

Fig. 1. (a) Fabrication process of the dual-wavelength DFB organic laser, (b) the tilt angle α of LC molecule under an electric field, and (c) schematic structure of the laser configuration with a grating period at 394 nm.

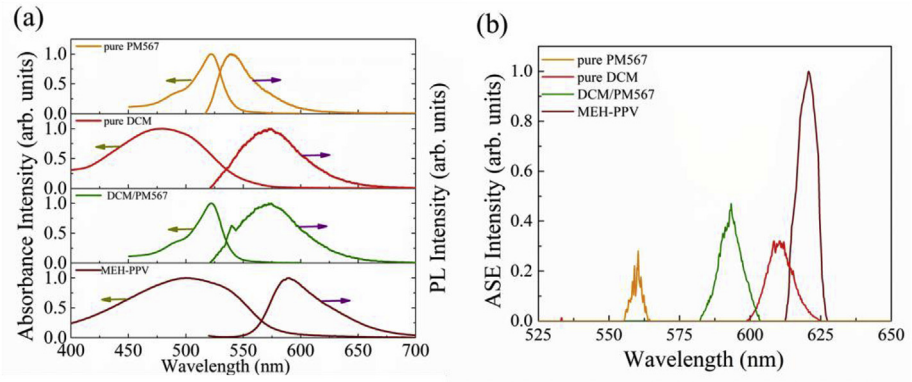

Fig. 2. Normalized intensity for (a) absorption and PL spectra, and (b) ASE spectra of pure PM567, pure DCM, DCM/PM567 and MEH-PPV film, respectively.

glass substrate in chlorobenzene (CB) solvent (8 mg ml^{-1}). The film thickness was controlled at ~80 nm. PI solution was spin-coated on another ITO glass substrate and rubbed along the z-axis. Then these two ITO glass substrates were prepared into an empty cell, and the cell gap was controlled by Mylar spacers at 6μm. The pre-polymer system consisted of 59 wt% monomer phthalic diglycol diacrylate (PDDA, Sigma-Aldrich), 28 wt% nematic liquid crystal TEB30A (n_o = 1.522, n_e = 1.692), 10 wt% cross-linker N-vinyl pyrrolidone (NVP, Sigma-Aldrich), extracted by Aldrich. Supplied), 1.5 wt% co-initiator N-phenylglycine (NPG, Sigma-Aldrich), 1.5 wt% photo-initiator Rose Bengal (RB, Sigma-Aldrich) and 0.1 wt% laser dyes. Three groups of laser dyes were adopted in our experiments: pure DCM (Sigma-Aldrich), pure PM567 (Sigma-Aldrich) and the blend DCM/PM567, at a weight ratio of 17:3.

In order to fabricate HPDLC grating, the empty cell injected with pre-polymer was exposed to two coherent and continuous s-polarized laser fields (laser wavelength:532 nm, intensity: 3.7 mW/cm^2) for 5 min. The grating period was carefully chosen at 394 nm, which depended on the angle between two coherent beams [23]. In order to study the optical properties of gain mediums, the absorption and photoluminescence (PL) spectra of the gain mediums were measured by a UV–Vis spectrophotometer (Shimadzu UV-3101; Shimadzu Corp., Japan) and fluorescence spectrophotometer (Hitachi F-7000; Hitachi, Ltd., Japan), respectively. The absorption and PL spectra of MEH-PPV can be measured by thin film spin-coated on glass substrate. While for dye blend or pure dye the absorption and PL spectra were measured by dyes-doped polymer dispersed liquid crystal (PDLC), which was fabricated by irradiating under a single laser beam from a Nd:YAG laser (532 nm, 10 mW/cm^{-2}) for 10 min.

The holographically cured sample was pumped by a Nd:YAG frequency doubled pulse laser (laser wavelength: 532 nm; pulse duration: 8 ns; repetition rate: 3 Hz). The pump beam was shaped into a 4 mm× 0.1 mm narrow stripe through a cylindrical lens and an adjustable slit. Then the narrow stripe was divided into two beams with equal intensity by a beam splitter prism. One beam was directly measured by an energy meter, and the other beam incident onto the sample at an angle of 45° with respect to the glass substrate. The dual-wavelength laser emission was perpendicular to the sample surface and was collected by a spectrometer (LabMax-TOP, Coherent Inc.). The schematic structure of the controllable dual-wavelength DFB laser is shown in Fig. 1c.

3. Results and discussion

3.1. Optical properties of gain medium

The Absorption and PL spectra of gain mediums were demonstrated in Fig. 2a. The absorption peak of pure PM567, pure DCM, DCM/PM567 and MEH-PPV film located at 522 nm, 478 nm and 522 nm,

500 nm, and their PL peaks located at and 540 nm, 575 nm, 572 nm and 589 nm, respectively. Specially, the absorption spectrum of the dye blend is similar to that of PM567, and the PL spectrum is similar to that of DCM. It is a clear indication of efficient Forster type energy transfer from the host dye PM567 to the guest dye DCM [24]. At the pump wavelength (532 nm), the absorption of dye blend is much stronger than pure DCM and the re-absorption loss is smaller than pure PM567. Therefore, the output lasing performance of dye blend is better than pure DCM and pure PM567.

We also measured the ASE spectra of gain mediums from PDLC layer at the same pump intensity, as shown in Fig. 2b. ASE locates at the maximum of the gain spectra, and it is a useful tool to explore lasing performance, such as the output lasing wavelength region and the threshold distribution at different wavelengths [25]. The ASE peaks of pure PM567, DCM/PM567, pure DCM, MEH-PPV located at 560.3 nm, 592.8 nm, 610.3 nm and 620.7 nm, respectively. The ASE intensity of the blend was higher than pure DCM and pure PM567, which indicated the blend had higher gain. The ASE of MEH-PPV film had the highest intensity, since it has no concentration quenching effect [26].

3.2. Dual-wavelength laser performance

When the pump energy is greater than the laser threshold, the laser emits a dual-wavelength laser. Fig. 3a is the spectra of the dual-wavelength laser measured at a pump energy of 0.60 μJ. The wavelengths obtained in one laser beam are 605.2 nm and 629.8 nm, respectively. The corresponding full width at half maximum (FWHM) is 0.5 nm and 0.4 nm. In order to distinguish the sources of these two wavelengths, the sample with the same parameters but no MEH-PPV layer was pumped. This indicates that the dye blend DCM/PM567 induce the 605.2 nm laser and the MEH-PPV layer leads to the 629.8 nm laser. The laser output wavelength satisfies the Bragg equation [27] $m\lambda = 2n_{eff}\Lambda$, in which n_{eff} is the effective refractive index, $\Lambda$is the grating period and m is the Bragg order, which is selected as 2 in this work. According to Bragg equation, the effective refractive index of laser emitted from DCM/PM567 and MEH-PPV is 1.54 and 1.60, respectively.

Fig. 3c shows the measurement results of polarization characteristics of the dual-wavelength laser. The lasers emitted from the sample are both TE polarization, but the reasons for this result are different. In our HPDLC gratings, the averaged orientation of LCs is aligned along the grating groove direction (z axis, as shown in Fig. 1c). The reason for this result is that only a difunctional acrylate monomer PDDA is utilized in this work. Low functional monomer will produce less polymer filaments in rich-LC regions due to the lower mobility, which exert less anchoring strength to LC molecules than the multifunctional functional monomer [28]. For the laser produced by dye blend DCM/PM567, the refractive index difference of TE polarized light comes from the polymer (n_p = 1.529) and the phase separated LCs (extraordinary index n_e = 1.692). Thus, the effective light feedback for TE polarized lasing output is high. However, the refractive index difference of TM polarized light comes from the polymer (n_p) and the phase separated LCs (ordinary index n_o = 1.522), the effective light feedback is much weaker. Therefore, the output laser induced by dyes DCM/PM567 only contained TE mode. The laser produced by MEH-PPV also only contains TE mode, but it is caused by waveguide theory. The refractive index of MEH-PPV layer is 1.90 in TE direction and1.52 in TM direction [29], while the refractive index is 1.54 in grating layer and 1.516 in glass substrate. For the asymmetric slab waveguide composed of HPDLC-grating/MEH-PPV/glass substrate, only TE mode light can be effectively bound in the resonator and amplified. Fig. 3d shows the

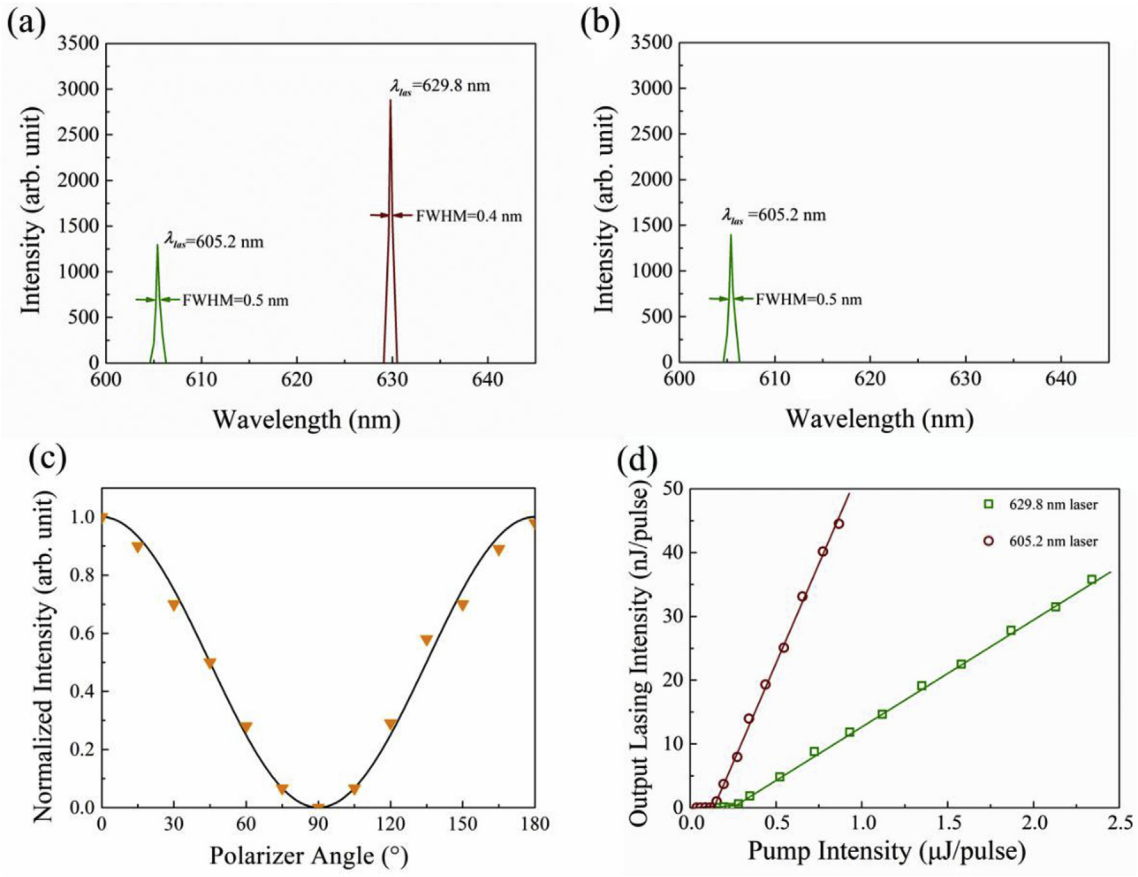

Fig. 3. Lasing spectra of (a) the dual-wavelength laser and (b) the single-wavelength without MEH-PPV layer at 0.70 μJ, (c) the transmitted intensity of the dual-wavelength laser on the dependence of the rotation angle, and (d) lasing output energy intensity as a function of pump energy of the dual-wavelength laser.

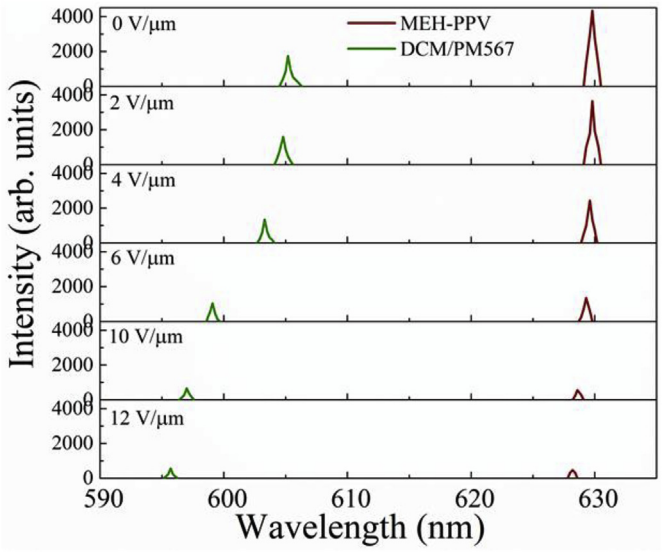

Fig. 4. Lasing spectra of the organic dual-wavelength laser under different electric fields.

dependence of output energy on the input energy of the dual-wavelength laser. The hollow points are experimental data, and the real lines are fitting data. The intersection point of the real line and the transverse axis is the threshold, and the slope of the real line is the conversion efficiency. The threshold is 0.14 μJ (i.e., pump energy density 0.035 mJ cm^{-2} or peak power density per pump laser pulse 4.34 kW cm^{-2}, the same as below) for the 629.8 nm MEH-PPV laser and 0.25 μJ (0.062 mJ cm^{-2} or 7.75 kW cm^{-2}) for the 605.2 nm dyes laser. The conversion efficiency of the lasers is 6.4% and 1.7%, respectively.

Compared with the dual-wavelength DFB laser generated by MEH-PPV and DCM with thresholds [22] of 0.16 μJ (0.053 mJ cm^{-2} or 6.7 kW cm^{-2}) and 0.36 μJ (0.12 mJ cm^{-2} or 15.0 kW cm^{-2}), the laser thresholds have been halved in this work. This result can be understood due to the following effects. One is from the phase separated LCs aligned along the rubbing direction (z axis). The refractive index difference for TE mode is greatly improved compared with the case of the phase separated LCs aligned along the grating vector. The bigger the refractive index in lasing feedback direction, the better the lasing feedback performance [28]. Therefore, the lasing threshold and conversion efficiency can be enhanced for both lasers in this work. Meanwhile, the lasing wavelength position of two laser beams is critical. The wavelength of the laser is located at the center of DCM/PM567 and MEH-PPV gain spectra respectively. The laser threshold will decrease significantly when the emission wavelength moves from the edge of the gain spectrum to the center, because of the higher gain and lower re-absorption effect [30]. Besides, for the dye blend laser, effective Forster energy transfer from PM567 to DCM also contributes to low threshold and high conversion efficiency.

3.3. Tunability by electric field

Fig. 4 shows the dual-wavelength laser tunable behaviors on the dependence of electric fields. The pumping energy density was measured at 0.8 μJ and kept constant for all electrical fields. When applied external electric field, the direction of LCs is shifted from z-axis to y-axis (as shown in Fig. 1b). The refractive index of TE polarized light in the LC layer changes from n_e to n_o. The decrease of the refractive index of HPDLC grating layer leads to the blue shift of lasers. Meanwhile, the refractive index difference of TE polarized light also decreases, which results in a decrease in the intensity of the output laser. Thus, as expected, the electrical control of the DFB organic dual-wavelength laser

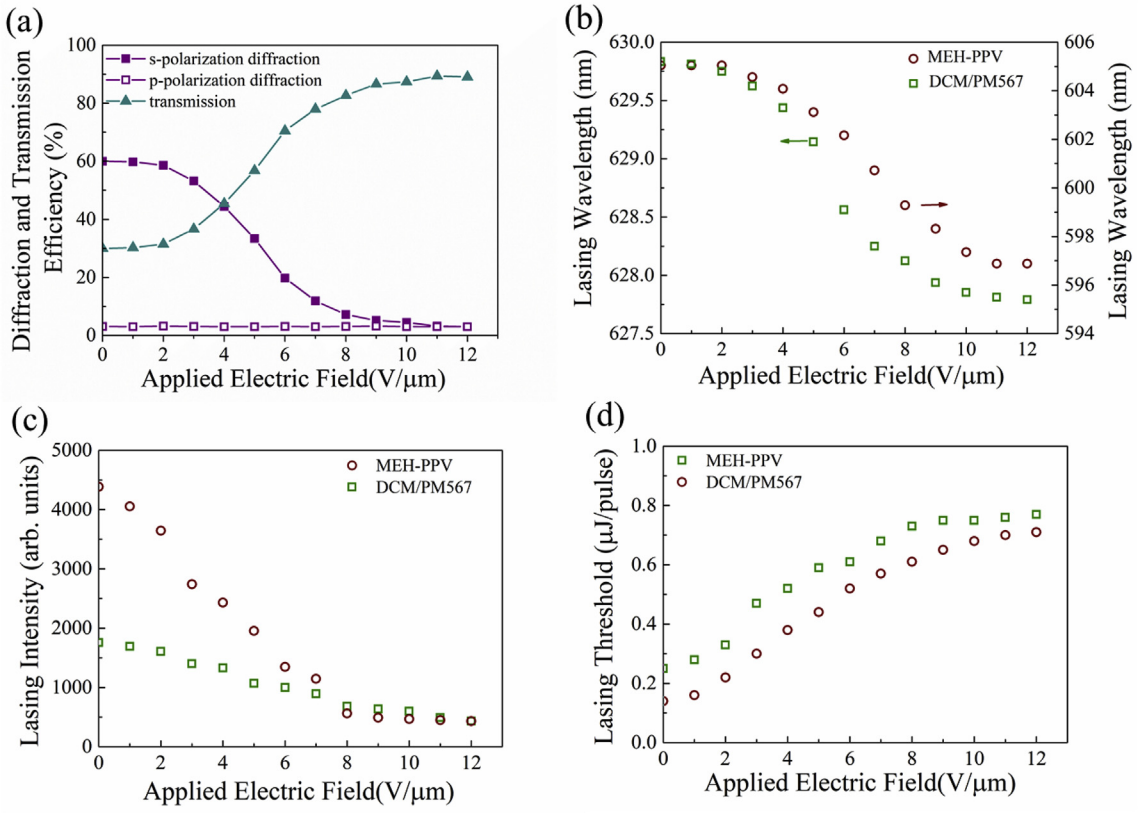

Fig. 5. (a) The diffraction efficiency for different polarizations and transmission efficiency, (b) lasing wavelength, (c) lasing intensity and (d) lasing thresholds under different electric fields.

is achieved. We can also predict that if the HPDLC gratings are fabricated by LCs with higher birefringence (the difference between n_e and n_o), the dual-wavelength tuning range can be further increased.

Fig. 5a shows the diffraction efficiencies in different polarization states and transmission efficiency under different electric fields. The diffraction efficiency for s-polarization is 60% higher than the one for p-polarization of 3% under no electric field, which proves again that the orientation of LCs is aligned along the rubbing direction (z axis). With the increase of external electric field, diffraction efficiency for s-polarization decreases, while diffraction efficiency for p-polarization remains unchanged. When applied voltage increases to 12 V/μm, diffraction efficiency for s-polarization no longer decreases, and it is equal to diffraction efficiency for p-polarization. The sum of diffraction efficiency and transmission efficiency is always 93%, which indicates that the scattering loss is about 7%. The lasers from MEH-PPV and dye blend blue shift 1.7 nm and 9.8 nm respectively with the electric field increased to 12 V/μm (as shown in Fig. 5b). The dual-wavelength lasing intensity decrease from 4385 to 432 (arb.units) for laser emitted from MEH-PPV and 1758 to 432 (arb.units) for laser from DCM/PM567 (as shown in Fig. 5c). The results of lasing wavelength and intensity are in good according with the change of diffraction efficiency of s-polarized light. Furthermore, the lasing thresholds under different electric fields were measured and shown in Fig. 5d. The lasing thresholds rise from 0.14 μJ (0.035 mJ cm^{-2} or 4.34 kW cm^{-2}) to 0.71 μJ (0.176 mJ cm^{-2} or 22.01 kW cm^{-2}) and 0.25 μJ (0.062 mJ cm^{-2} or 7.75 kW cm^{-2}) to 0.77 μJ (0.191 mJ cm^{-2} or 23.87 kW cm^{-2}) for lasers from MEH-PPV and dye blend, respectively. It is another sign of the decrease in refractive index difference between polymer and the phase separated LCs, because a lower refractive index difference always leads to a higher lasing threshold.

4. Conclusions

In conclusion, we have presented a surface-emitting dual-wavelength laser from dye blend and organic semiconductor with a HPDLC grating feedback structure. The performance for both lasers has been greatly improved by adopting PI layer and effective Forster energy transfer. Although the working mechanism is different, the lasers emitted from the sample are both TE polarization. The tuning characteristics of dual-wavelength laser under external electric field are further studied. The modulated lasing intensity and wavelength are attributed to the decreases in the refractive index difference and average refractive index of the HPDLC grating respectively. Therefore, we think that this work would widen the applications of DWLs in the field of laser displays and integrated photonic circuits and more work to further enhance the tunable range is ongoing.

Acknowledgements

The authors would like to thank the support from financial support from National Natural Science Foundation of China (Grant No. 51702185), Natural Science Foundation of Shandong Province (Grant Nos. ZR2017BEM029, ZR2017MD019).

References

[1] M. Maiwald, J. Fricke, A. Ginolas, J. Pohl, B. Sumpf, G. Erbert, G. Tränkle, Dual-wavelength monolithic Y-branch distributed Bragg reflection diode laser at 671 nm suitable for shifted excitation Raman difference spectroscopy, Laser Photonics Rev. 7 (2013) L30–L33.
[2] C.-L. Wang, Y.-H. Chuang, C.-L. Pan, Two-wavelength interferometer based on a two-color laser-diode array and the second-order correlation technique, Opt. Lett. 20 (1995) 1071–1073.
[3] H.H. Telle, A.G. Ureña, R.J. Donovan, Laser Chemistry: Spectroscopy, Dynamics and Applications, John Wiley & Sons, 2007.
[4] N. Pavel, Simultaneous dual-wavelength emission at 0.90 and 1.06 μm in Nd-doped laser crystals, Laser Phys. 20 (2010) 215–221.
[5] L. Fan, M. Fallahi, J. Hader, A.R. Zakharian, J.V. Moloney, W. Stolz, S.W. Koch, R. Bedford, J.T. Murray, Linearly polarized dual-wavelength vertical-external-cavity surface-emitting laser, Appl. Phys. Lett. 90 (2007) 181124.
[6] L. Guo, R. Lan, H. Liu, H. Yu, H. Zhang, J. Wang, D. Hu, S. Zhuang, L. Chen, Y. Zhao, 1319 nm and 1338 nm dual-wavelength operation of LD end-pumped Nd: YAG ceramic laser, Optic Express 18 (2010) 9098–9106.
[7] I.D.W. Samuel, G.A. Turnbull, Organic semiconductor lasers, Chem. Rev. 107 (2007) 1272–1295.
[8] B.J. Scott, G. Wirnsberger, M.D. McGehee, B.F. Chmelka, G.D. Stucky, Dye-doped mesostructured silica as a distributed feedback laser fabricated by soft lithography, Adv. Mater. 13 (2001) 1231–1234.
[9] D. Amarasinghe, A. Ruseckas, G.A. Turnbull, I.D.W. Samuel, Organic semiconductor optical amplifiers, Proc. IEEE 97 (2009) 1637–1650.
[10] G. Zhang, L. Liu, M. Liu, Y. Liu, Z. Peng, L. Yao, Q. Wang, S. Wang, Z. Cao, J. Ma, L. Xuan, Tunable surface-emitting dual-wavelength laser from a blended gain layer with an external holographic grating feedback structure, Opt. Mater. Express 6 (2016) 3320.
[11] Z. Diao, S. Deng, W. Huang, L. Xuan, L. Hu, Y. Liu, J. Ma, Organic dual-wavelength distributed feedback laser empowered by dye-doped holography, J. Mater. Chem. 22 (2012) 23331.
[12] S. Klinkhammer, N. Heussner, K. Huska, T. Bocksrocker, F. Geislhöringer, C. Vannahme, T. Mappes, U. Lemmer, Voltage-controlled tuning of an organic semiconductor distributed feedback laser using liquid crystals, Appl. Phys. Lett. 99 (2011) 023307.
[13] F.J. Duarte, Tunable Laser Applications, CRC Press, New York, 2009.
[14] W. Huang, Z. Diao, L. Yao, Z. Cao, Y. Liu, J. Ma, L. Xuan, Electrically tunable distributed feedback laser emission from scaffolding morphologic holographic polymer dispersed liquid crystal grating, Appl. Phys. Express 6 (2013) 022702.
[15] H. Coles, S. Morris, Liquid-crystal lasers, Nat. Photon. 4 (2010) 676–685.
[16] M. Wang, C. Zou, C. Li, J. Sun, L. Wang, W. Hu, C. Zhang, L. Zhang, W. He, H. Yang, Bias-Polarity dependent bidirectional modulation of photonic bandgap in a nanoengineered 3D blue phase polymer scaffold for tunable laser application, Adv. Opt. Mater. 6 (2018) 1800409.
[17] M. Wang, C. Zou, J. Sun, L. Zhang, L. Wang, J. Xiao, F. Li, P. Song, H. Yang, Asymmetric tunable photonic bandgaps in self-organized 3D nanostructure of polymer-stabilized blue phase I modulated by voltage polarity, Adv. Funct. Mater. 27 (2017) 1702261.
[18] D. Luo, X.W. Sun, H.T. Dai, H.V. Demir, H.Z. Yang, W. Ji, Electrically tunable lasing from a dye-doped two-dimensional hexagonal photonic crystal made of holographic polymer-dispersed liquid crystals, Appl. Phys. Lett. 97 (2010) 081101.
[19] W. Huang, Y. Liu, Z. Diao, C. Yang, L. Yao, J. Ma, L. Xuan, Theory and characteristics of hologr aphic polymer dispersed liquid crystal transmiss ion grating, Appl. Opt. 51 (2012) 4013.
[20] R. Jakubiak, V.P. Tondiglia, L.V. Natarajan, R.L. Sutherland, P. Lloyd, T.J. Bunning, R.A. Vaia, Dynamic lasing from all-organic two-dimensional photonic crystals, Adv. Mater. 17 (2005) 2807–2811.
[21] M. Liu, Y. Liu, G. Zhang, L. Liu, Z. Diao, C. Yang, Z. Peng, L. Yao, J. Ma, L. Xuan, Improving the conversion efficiency of an organic distributed feedback laser by varying solvents of the laser gain layer, Liq. Cryst. (2016) 1–10.
[22] Z. Diao, L. Xuan, L. Liu, M. Xia, L. Hu, Y. Liu, J. Ma, A dual-wavelength surface-emitting distributed feedback laser from a holographic grating with an organic semiconducting gain and a doped dye, J. Mater. Chem. C 2 (2014) 6177.
[23] L. Liu, L. Xuan, J. Ma, Optical Performance of Organic Distributed Feedback Lasers Based on Holographic Polymer Dispersed Liquid Crystals, Springer, London, 2016, pp. 379–405.
[24] L. Liu, W. Huang, Z. Diao, Z. Peng, Q. q. Mu, Y. Liu, C. Yang, L. Hu, L. Xuan, Low threshold of distributed feedback lasers based on scaffolding morphologic holographic polymer dispersed liquid crystal gratings: reduced losses through Forster transfer, Liq. Cryst. 41 (2013) 145–152.
[25] K. Kretsch, C. Belton, S. Lipson, W. Blau, F. Henari, Amplified spontaneous emission and optical gain spectra from stilbenoid and phenylene vinylene derivative model compounds, J. Appl. Phys. 86 (1999) 6155–6159.
[26] M.D. McGehee, A.J. Heeger, Semiconducting (conjugated) polymersas materials for solid-state lasers, Adv. Mater. 12 (2000) 1655–1668.
[27] H. Kogelnik, C.V. Shank, CoupledWave theory of distributed feedback lasers, J. Appl. Phys. 43 (1972) 2327–2335.
[28] L. Lijuan, X. Li, Z. Guiyang, L. Minghuan, H. Lifa, L. Yonggang, M. Ji, Enhancement of pump efficiency for an organic distributed feedback laser based on a holographic polymer dispersed liquid crystal as an external light feedback layer, J. Mater. Chem. C 3 (2015) 5566–5572.
[29] M. Tammer, A.P. Monkman, Measurement of the anisotropic refractive indices of spin cast thin poly(2-methoxy-5-(2-ethyl-hexyloxy)-p-phenyl-enevinylene) (MEH-PPV) films, Adv. Mater. 14 (2002) 210–212.
[30] G. Heliotis, R. Xia, G.A. Turnbull, P. Andrew, W.L. Barnes, I.D.W. Samuel, D.D.C. Bradley, Emission characteristics and performance comparison of polufluorene lasers with one- and two-dimensional distributed feedback, Adv. Funct. Mater. 14 (2004) 91–97.